Nitronyl Nitroxide Biradicals as Tetradentate Chelates: Unusually Large Metal−Nitroxide Ferromagnetic Interactions

Dominique Luneau,*,† Francisco M. Romero,‡ and Raymond Ziessel*,‡

Département de Recherche Fondamentale sur la Matière Condensée, Service de Chimie Inorganique et Biologique, Laboratoire de Chimie de Coordination (URA CNRS 1194), CEA-Grenoble, 38054 Grenoble, France, and Laboratoire de Chimie, d'Électronique et de Photonique Moléculaires, École de Chimie, Polymères et Matériaux, UPRES-A 7008, 1 Rue Blaise Pascal, 67008 Strasbourg, France

Received March 25, 1998

A series of mononuclear transition metal complexes of the tetradentate (N_2O_2) 6,6′-bis(3″-oxide-1″-oxyl-4″,4″,5″,5″-tetramethylimidazoline-2″-yl)-2,2′-bipyridine (NIT-bpy) has been prepared and characterized by spectroscopic, magnetic, and single-crystal X-ray diffraction studies. The free NIT-bpy ligand is planar with an anti-conformation, whereas in each complex this ligand is tetracoordinated to the metal in a syn-conformation comprising the equatorial plane of a distorted octahedron. Complexes differ by the nature of the ancillary ligands occupying the trans-axial positions, these being two water molecules in $[Ni^{II}(NIT\text{-}bpy)\cdot 2H_2O](ClO_4)_2$, **1**, one molecule of water and one perchlorate anion in $[M(NIT\text{-}bpy)\cdot H_2O\cdot ClO_4]ClO_4$ (M = Ni(II), **2**; Mn(II), **3**; Co(II), **4**), or two perchlorate anions in $[Cu^{II}(NIT\text{-}bpy)\cdot 2ClO_4]$, **5**. The ferromagnetic metal−nitroxide coupling found for the nickel complex **1** ($J_{12} = +39.6$ cm^{-1}) arises from near-coplanarity between the π-conjugated radical plane and the equatorial plane of the *trans*-diaqua$\{Ni(N_2O_2)(H_2O)_2\}$ octahedron. Deviations from this geometry lead to antiferromagnetic components that are dominant in complex **1** ($J_{23} = -48.7$ cm^{-1}) and tend to reduce the extent of the ferromagnetic interactions in complex **2** ($J_{12} = +27.8$ cm^{-1} and $J_{23} = +6.9$ cm^{-1}). For the Mn^{2+} complex **3**, variable temperature studies indicate antiferromagnetic behavior $J = -65.3$ cm^{-1}, but with weak intermolecular ferromagnetic interactions $zJ' = +0.22$ cm^{-1}. For the Co^{2+} complex **4**, experimental data were best explained as a weak ferromagnetic interaction $J_{12} = +0.40$ cm^{-1} and a relatively strong antiferromagnetic interaction $J_{23} = -28.0$ cm^{-1}. The Cu^{2+} complex **5** exhibits strong antiferromagnetic behavior $J = -166.8$ cm^{-1}. The magnetic data of the $[M'(NIT\text{-}bpy)](ClO_4)_2$ (M′ = Zn(II), **6**; Fe(II) low-spin, **7**) complexes were fit to a Curie−Weiss law ($\theta = -2.43$ cm^{-1} for **6** and $\theta = -0.51$ cm^{-1} for **7**). No intramolecular radical−radical interaction is apparent in any of these complexes.

Introduction

The engineering of molecular magnets constitutes a major contemporary research aim and has spawned interest in organic radicals as building blocks for the construction of new materials.[1,2] Purely organic polycarbenes,[3] halogenated polyradicals,[4] and fullerene-based charge-transfer derivatives[5] give rise to interesting magnetic properties, but most are too reactive to be well characterized. Organic radicals have also been used in conjunction with paramagnetic transition metal ions. Typical examples are tetracyanoethylene complexes of decamethylferrocenium[6] and *meso*-tetraphenylporphinatomanganese(II)[7] and -vanadium(II),[8] for which strong magnetic coupling results in the onset of ferromagnetism well above room temperature. In some cases (e.g. semiquinonate complexes) the metal center serves to stabilize the radical.[9,10]

Many different types of stable organic radicals have been studied so far. One of the more popular families concerns the nitronyl nitroxide radicals.[11] The synthesis and electronic properties of this family were pioneered by Ullman nearly 20 years ago.[12] At that time, research was largely motivated by the use of nitroxides and nitronyl nitroxides as spin probes in an effort to obtain structural information for biological systems.[13] In the 1990s the γ-crystal phase of the *p*-nitrophenyl nitronyl nitroxide radical was found to behave as an organic ferromag-

† CEA-Grenoble.
‡ ECPM.

(1) Kahn, O. *Molecular Magnetism*; VCH: New York, 1993.
(2) Coronado, E., Delhaès, P., Gatteschi, D., Miller, J. S., Eds. *Molecular Magnetism: From Molecular Assemblies to the Devices*; NATO ASI Series 321; Kluwer Academic Publishers: Dordrecht, 1996.
(3) Nakamura, N.; Inoue, K.; Iwamura, H. *Angew. Chem., Int. Ed. Engl.* **1993**, *32*, 872.
(4) Veciana, J.; Rovira, C.; Ventosa, N.; Crespo, M. I.; Palacio, F. *J. Am. Chem. Soc.* **1993**, *115*, 57.
(5) Allemand, P. M.; Khemani, K. C.; Koch, A.; Wudl, F.; Holczer, K.; Donovan, S.; Grüner, G.; Thompson, J. D. *Science* **1991**, *259*, 303.
(6) Miller, J. S.; Calabrese, J. C.; Rommelmann, H.; Chittipeddi, S. R.; Zhang, J. H.; Reiff, W. M.; Epstein, A. J. *J. Am. Chem. Soc.* **1987**, *109*, 769.
(7) Miller, J. S.; Calabrese, J. C.; McLean, R. S.; Epstein, A. J. *Adv. Mater.* **1992**, *4*, 498.
(8) Manriquez, J. M.; Yee, G. T.; McLean, R. S.; Epstein, A. J.; Miller, J. S. *Science* **1991**, *252*, 1415.
(9) Benelli, C.; Dei, A.; Gatteschi, D.; Gudel, H. U.; Pardi, L. *Inorg. Chem.* **1989**, *28*, 3089.
(10) Adams, D. M.; Dei, A.; Rheingold, A. L.; Hendrickson, D. N. *Angew. Chem., Int. Ed. Engl.* **1993**, *32*, 880.
(11) Ullman, E. F.; Osiecki, J. H.; Boocock, D. G. B.; Darcy, R. *J. Am. Chem. Soc.* **1972**, *94*, 7049.
(12) Ullman, E. F.; Call, L.; Leute, R. K.; Osieki, J. H. U.S. Patent 3,740,412, 1973.
(13) Keana, J. F. W. *Chem. Rev.* **1978**, *78*, 37.

S0020-1669(98)00341-3 CCC: $15.00
Published on Web 09/15/1998

net.[14] This very rare behavior has stimulated the present attraction of chemists for persistent organic free radicals, and indeed ferromagnetic ordering at very low temperatures has been discovered in other organic compounds.[15−19]

One of the most interesting aspects of stable organic radicals is their chemical versatility since this provides for a variety of molecular assemblies when coordinated to transition metals.[20,21] Metal ions bound directly to nitronyl nitroxide monoradicals are also shown to give one-dimensional ferrimagnets which order ferromagnetically at low temperature. Many different molecular arrangements have been found by coordination of nitronyl nitroxide free radicals to transition metal complexes, including (i) discrete molecules obtained by coordination to a single metal atom,[22,23] (ii) linear chains formed by bridging two individual metal complexes with a bidentate nitronyl nitroxide radical,[24,25] (iii) polymeric ladder compounds formed with a tridentate nitronyl nitroxide radical,[26] and (iv) discrete molecules of a cyclic manganese hexamer with 12 coupled spins and $S = 12$ ground state.[27] Recently, ferrimagnetic ordering in manganese(II) bis(hexafluoroacetylacetonate) complexes formed with tertiobutyl-nitroxide triradicals has been observed.[28−30]

Most of the systems studied to date use strongly acidic metal ions (e.g. hexafluoroacetylacetonates) to coordinate the weakly basic *N*-oxide *N*-oxyl to the metal center.[31] In an effort to use classical paramagnetic salts to increase intermolecular interactions and to expand dimensionality, attention has turned to free nitronyl nitroxyde monoradicals bearing nitrogen heteroaromatics. Archetypal examples are pyridine,[32,33] pyridinium salts,[34] ethynylpyridine,[19,35] quinoline,[36] pyrimidine,[37] pyrazine,[38] imidazole[39] and 1,2,4-triazole derivatives.[40,41] Pyridine and oligopyridine biradicals (2,6-pyridine, 2,5-pyridine, 2,2′-bipyridine, 1,10-phenanthroline, 3,6-pyridazine, 2,8-naphthyridine)[42−44] have also been investigated, and, in particular, α,α′-disubstituted 2,2′-bipyridine or 1,10-phenanthroline residues behave as a semirigid molecular tweezer that holds the two radicals in a cis configuration when coordinated to a transition metal.[45] We now report that this tetradentate coordinative mode of the ligand orientates the magnetic orbitals, and thereby controls the extent of metal−radical interaction. In some cases, complexation forces the magnetic orbitals to be orthogonal, resulting in the appearance of large ferromagnetic interactions. This is discussed in a series of complexes comprising the preorganized NIT-bpy spin-carrier and diamagnetic Fe(II) and Zn(II) or paramagnetic Cu(II), Ni(II), Co(II), and Mn(II) ions. It should also be noted that this polydentate ligand avoids the use of strongly acidic paramagnetic metal centers.

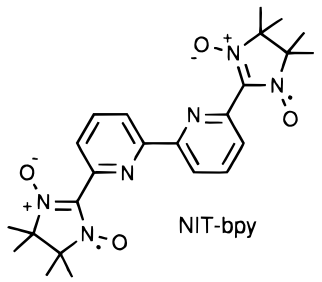

Experimental Section

(A) X-ray Crystal Structure Analysis. The intensity data were collected in the $\omega-2\theta$ mode, at room temperature, on an Enraf-Nonius CAD4 diffractometer equipped with a graphite monochromator for the Mo Kα ($\lambda = 0.7109$ Å) radiation. Cell constants were derived from a least-squares fit of the setting angles for 25 selected reflections with $10° \leq \theta \leq 15°$. The intensities were corrected for Lorentz and polarization effects but not for absorption. The positions of the metal ions were found using the SHELX86 package.[47] The remaining atoms were located in a succession of difference Fourier syntheses and were refined with anisotropic thermal parameters using the SHELX76 package.[48] The hydrogen atoms were included in the final refinement model in calculated and fixed positions with isotropic thermal parameters. During structure refinement of compound **1**, the atom positions of one of the two nitronyl nitroxide fragments was found to be disordered, resulting in the large esd on distances and angles and the relatively high *R* value. All our efforts to improve the structure quality, including splitting of the disordered atoms and low temperatures

(14) Kinoshita, M.; Turek, P.; Tamura, M.; Nozawa, K.; Shiomi, D.; Nakazawa, Y.; Ishikawa, M.; Takahashi, M.; Awaga, K.; Inabe, T.; Maruyama, Y. *Chem. Lett.* **1991**, 1225.
(15) Chiarelli, R.; Novak, M. A.; Rassat, A.; Tholence, J. L. *Nature* **1993**, 363, 147.
(16) Nogami, T.; Ishida, T.; Tsuboi, H.; Yoshikawa, H.; Yamamoto, H.; Yasui, M.; Iwasaki, F.; Iwamura, H.; Takeda, N.; Ishikawa, M. *Chem. Lett.* **1995**, 635.
(17) Cirujeda, J.; Mas, M.; Molins, E.; L. De Panthou, F.; Laugier, J.. Park, G. P.; Paulsen, C.; Rey, P.; Rovira, C.; Veciana, J. *J. Chem. Soc., Chem. Commun.* **1995**, 709.
(18) Caneschi, A.; Ferraro, F.; Gatteschi, D.; Le Liszin, A.; Novak, M. A.; Rentschler, E.; Sessoli, R. *Adv. Mater.* **1995**, *7*, 476.
(19) Romero, F. M.; Ziessel, R.; Drillon, M.; Tholence, J.-L.; Paulsen, C.; Kyritsakas, N.; Fischer, J. *Adv. Mater.* **1996**, *8*, 826.
(20) Caneschi, A.; Gatteschi, D.; Sessoli, R.; Rey, P. *Acc. Chem. Res*. **1989**, *22*, 392.
(21) Caneschi, A.; Gatteschi, D.; Rey, P. *Prog. Inorg. Chem.* **1991**, *39*, 331.
(22) Gatteschi, D.; Laugier, J.; Rey, P.; Zanchini, C. *Inorg. Chem*. **1987**, *26*, 938.
(23) Benelli, C.; Caneschi, A.; Gatteschi, D.; Pardi, L. *Inorg. Chem*. **1992**, *31*, 741.
(24) Caneschi, A.; Gatteschi, D.; Laugier, J.; Rey, P. *J. Am. Chem. Soc*. **1987**, *109*, 2191.
(25) Luneau, D.; Rey, P.; Laugier, J.; Fries, P.; Caneschi, A.; Gatteschi, D.; Sessoli, R. *J. Am. Chem. Soc.* **1991**, *113*, 1245.
(26) Caneschi, A.; Ferraro, F.; Gatteschi, D.; Rey, P.; Sessoli, R. *Inorg. Chem*. **1991**, *30*, 3162.
(27) Caneschi, A.; Gatteschi, D.; Laugier, J.; Rey, P.; Sessoli, R.; Zanchini, C. *J. Am. Chem. Soc.* **1988**, *110*, 2795.
(28) Inoue, K.; Iwamura, H. *J. Am. Chem. Soc.* **1994**, *116*, 3173.
(29) Inoue, K.; Iwamura, H. *Adv. Mater.* **1996**, *8*, 73.
(30) Inoue, K.; Hayamizu, T.; Iwamura, H.; Hashizume, D.; Ohashi, Y. *J. Am. Chem. Soc.* **1996**, *118*, 1803.
(31) Caneschi, A.; Ferraro, F.; Gatteschi, D.; Rey, P.; Sessoli R. *Inorg. Chem.* **1990**, *29*, 1756 and references therein.
(32) Caneschi, A.; Ferraro, F.; Gatteschi, D.; Rey, P.; Sessoli, R. *Inorg. Chem.* **1990**, *29*, 4217.
(33) Luneau, D.; Risoan, G.; Rey, P.; Grand, A.; Caneschi, A.; Gatteschi, D.; Laugier, J. *Inorg. Chem*. **1993**, *32*, 5616.
(34) Awaga, K.; Inabe, T.; Nakamura, T.; Matsumoto, M.; Maruyama, Y. *Mol. Cryst. Liq. Cryst*. **1993**, *232*, 69.
(35) Romero, F. M.; Ziessel, R.; De Cian, A.; Fischer, J.; Turek, P. *New J. Chem*. **1996**, *20*, 919.
(36) Sugano, T.; Tamura, M.; Goto, T.; Kato, R.; Kinoshita, M.; Sasaki, Y.; Kurmoo, M.; Day, P. *Mol. Cryst. Liq. Cryst*. **1993**, *232*, 61.
(37) L. De Panthou, F.; Luneau, D.; Laugier, J.; Rey, P. *J. Am. Chem. Soc.* **1993**, *115*, 9095.
(38) Luneau, D.; Rey, P. *Magnetism: A Supramolecular Function*; Kahn, O., Ed.; NATO ASI Series 484; Kluwer Academic Publishers: Dordrecht, 1996; p 431.
(39) Luneau, D.; Rey, P. *Mol. Cryst. Liq. Cryst*. **1995**, *273*, 81.
(40) Pei, Y.; Kahn, O.; Aebersold, M. A.; Ouahab, L.; Le Berre, F.; Pardi, L.; Tholence, J. L. *Adv. Mater*. **1994**, 6, 681.
(41) Lang, A.; Pei, Y.; Ouahab, L.; Kahn, O. *Adv. Mater*. **1996**, 8, 60.
(42) Ulrich, G.; Ziessel, R.; Luneau, D.; Rey, P. *Tetrahedron Lett*. **1994**, *35*, 1211.
(43) Ulrich, G.; Ziessel, R. *Tetrahedron Lett*. **1994**, *35*, 1215.
(44) Ziessel, R. *Mol. Cryst. Liq. Cryst*. **1995**, *273*, 101.
(45) Luneau, D.; Laugier, J.; Rey, P.; Ulrich, G.; Ziessel, R.; Legoll, P.; Drillon, M. *J. Chem. Soc., Chem. Commun.* **1994**, 741.
(46) Romero, F.; Luneau, D.; Ziessel, R. *J. Chem. Soc., Chem. Commun.* **1998**, 551.
(47) Sheldrick, G. M. *Crystallographic Computing 3*; Sheldrick, G. M., Kruger, C., Goddard, R., Eds.; Oxford University Press: Oxford, U.K., 1985; p 175.
(48) Sheldrick, G. *System of Computing Programs*; University of Cambridge: Cambridge, England, 1976.

Table 1. Summary of the Crystal Structure Data Collection and Refinement for **1**−**4**

	1	**2**	**3**	**4**
empirical formula	$C_{24}H_{34}N_6O_{14}Cl_2Ni$	$C_{26}H_{35}N_7O_{13}Cl_2Ni$	$C_{26}H_{35}N_7O_{13}Cl_2Mn$	$C_{26}H_{35}N_7O_{13}Cl_2Co$
fw	760.18	783.21	779.44	783.43
temp (K)	293	293	293	293
cryst syst	triclinic	monoclinic	monoclinic	monoclinic
space group	$P\bar{1}$	$P2_1/c$	$P2_1/c$	$P2_1/c$
Z	2	4	4	4
a (Å)	8.501(2)	10.732(3)	10.978(3)	10.801(3)
b (Å)	12.815(3)	20.823(3)	21.189(3)	20.935(3)
c (Å)	16.086(3)	14.742(3)	14.681(3)	14.743(3)
α (deg)	87.35(1)			
β (deg)	84.86(1)	93.22(1)	94.54(1)	93.53(1)
γ (deg)	71.18(1)			
V (Å^3)	1651.78	3289.2	3404.3	3327.35
D_c (g cm^{-3})	1.529	1.581	1.521	1.564
μ(Mo Kα) (cm^{-1})	8.25	7.85	7.58	7.10
λ (Å)	0.710 73	0.710 73	0.710 73	0.710 73
weight	$1/\sigma^2$	$1/\sigma^2$	$1/\sigma^2$	$1/\sigma^2$
GOF[a]	1.30	0.900	1.04	1.20
$R(F_o)$[b]	0.0747	0.0417	0.0689	0.0543
$R_w(F_o)$[c]	0.0705	0.0369	0.0671	0.0536

[a] GOF = $[\Sigma w(|F_o|^2 - |F_c|^2)2/(n-p)]^{1/2}$. [b] $R(F_o) = \Sigma(|F_o| - |F_c|)/\Sigma|F_o|$. [c] $R_w(F_o) = \Sigma(w^{1/2}|F_o| - |F_c|)/\Sigma w^{1/2}|F_o|$.

studies, were unsuccessful. Crystal structure and refinement data are summarized in Table 1 for compounds **1** and the isostructural compounds **2**−**4**.

(B) Magnetic Susceptibility Measurements. The magnetic susceptibility was measured on the bulk material in the 2−300 K temperature range for each compound and also on a frozen solution[49] for the free radical with a Quantum Design MPMS superconducting SQUID magnetometer operating at field strength of 5 kOe or with a M 8100 SQUID susceptometer Métronique at field strength of a few kOe. The data were corrected for magnetization of the sample holder and the magnetic susceptibility was corrected for diamagnetism of the constituent atoms using Pascal constants.

(C) Materials. 2,3-Bis(hydroxylamino)-2,3-dimethylbutane,[50] and 6,6′-diformyl-2,2′-bipyridine,[51] and the NIT-bpy ligand[45] were prepared according to literature procedures. Perchlorate salts were used as purchased.

CAUTION: *Note that perchlorate salts should be handled carefully, in low quantities, used as hydrated salts, and never dehydrated under vacuum before used.*

(a) Preparation of Complexes 1 and 5. Stoichiometric amounts of NIT-bpy (100 mg scale) and $M(ClO_4)_2{\cdot}6H_2O$ (M = Ni, Cu) were mixed in methanol. The resultant green solution was filtered and evaporated slowly. After a few days of standing, platelike crystals were isolated.

(b) Complexes 2−4, 6, and 7. Stoichiometric amounts of NIT-bpy (100 mg scale) in dichloromethane (10 mL) and $M(ClO_4)_2{\cdot}6H_2O$ (M = Ni, Mn, Co, Zn, Fe) in ethyl acetate (10 mL) were mixed, affording a fast color change from blue to green as a consequence of complexation of the metal by the "tweezer" ligand. Stirring the solution for 10 min led to quantitative precipitation of the complex, which was recovered by centrifugation and washed with ethyl acetate and diethyl ether. Recrystallization by slow evaporation of acetonitrile from a solution of acetonitrile/toluene (ca 1/1) gave well-formed single crystals of the desired complex. The iron(II) complex was prepared using vacuum line and Schlenk tube techniques and argon-distilled solvents. This complex must be stored in the absence of oxygen. All complexes were analyzed in the form of powders.

[Ni(NIT-bpy)·2H$_2$O](ClO$_4$)$_2$ (1). 75%; FAB$^+$ (*m*-NBA)) 623.1 [M − ClO_4]$^+$, 609.2 [M − ClO_4 + 2H − O], 592.1 [M − ClO_4 + H − 2O], 525.2 [M − 2ClO_4 + H], 508.2 [M − 2ClO_4−O], 492.2 [M − 2ClO_4 − 2O], 478.2 [M − 2ClO_4 − 2O]; IR (KBr pellet, cm^{-1}) 1594 (m), 1425 (m), 1350 (s) (ν_{NO}), 1144 (s), 1115 (s), 1088 (s), 807 (m), 625 (m); UV (CH_3CN) λ (nm) (ϵ (M^{-1} cm^{-1})) 699 (210), 588 (560) ($n \rightarrow \pi^*$, NO), 382 (12 200), 336 (21 900), 215 (36 700). Anal. Calcd for $C_{24}H_{30}O_{12}N_6Cl_2Ni{\cdot}2H_2O$ (M_r = 724.146 + 36.031): C, 37.92; H, 4.51; N, 11.06. Found: C, 38.80; H, 4.42; N, 10.74.

[Ni(NIT-bpy)·H$_2$O·ClO$_4$](ClO$_4$), CH$_3$CN (2). 88%; FAB$^+$ (*m*-NBA) 625.2 [M − ClO_4 + 2H]$^+$, 609.1 [M − ClO_4 + 2H − O], 593.2 [M − ClO_4 + 2H − 2O], 525.1 [M − 2ClO_4 + H], 509.1 [M − 2ClO_4 + H − O], 492.1 [M − 2ClO_4 − 2O]; IR (KBr pellet, cm^{-1}) 2978 (m), 1594 (m), 1425 (m), 1354 (s), 1268 (m), 1200 (m), 1143 (s), 1117 (s), 1087 (s), 1048 (s), 813 (m), 637 (m), 627 (m); UV (CH_3CN) λ (nm) (ϵ (M^{-1}cm^{-1})) 699 (330), 587 (770), 383 (14 100), 334 (25 300), 273 (19 600). Anal. Calcd for $C_{24}H_{30}O_{12}N_6Cl_2Ni{\cdot}CH_3CN{\cdot}H_2O$ (M_r = 724.146 + 41.052 + 18.015): C, 39.87; H, 4.50; N, 12.52. Found: C, 40.73; H, 4.26; N, 12.45.

[Mn(NIT-bpy)·H$_2$O·ClO$_4$](ClO$_4$), CH$_3$CN (3). 98%; FAB$^+$ (*m*-NBA) 640.2 [M − ClO_4 + 2H]$^+$, 624.2 [M − ClO_4 + 2H − O], 608.1 [M − ClO_4 + 2H − 2O], 540.2 [M − 2ClO_4 + H], 524.2 [M − 2ClO_4 + H − O], 507.1 [M − 2ClO_4 − 2O]; IR (KBr pellet, cm^{-1}) 1592 (m), 1430 (m), 1350 (s) (ν_{NO}), 1260 (m), 1196 (m), 1141 (s), 1115 (s), 1085 (s), 808 (m), 625 (m); UV (CH_3CN) λ (nm) (ϵ (M^{-1} cm^{-1})) 670 (470), 576 (800), 372 (8800), 332 (16 200), 273 (12 100). Anal. Calcd for $C_{24}H_{30}O_{12}N_6Cl_2Mn{\cdot}CH_3CN{\cdot}H_2O$ (M_r = 720.384 + 41.052 + 18.015): C, 40.07; H, 4.53; N, 12.58. Found: C, 40.95; H, 4.21; N, 12.68.

[Co(NIT-bpy)·H$_2$O·ClO$_4$](ClO$_4$), CH$_3$CN (4). 93%; FAB$^+$ (*m*-NBA) 644.1 [M − ClO_4 + 2H]$^+$, 628.1 [M − ClO_4 + 2H − O], 612.1 [M − ClO_4 + 2H − 2O], 544.3 [M − 2ClO_4 + H], 528.3 [M − 2ClO_4 + H − O], 511.2 [M − 2ClO_4 − 2O]; IR (KBr pellet, cm^{-1}) 1595 (m), 1455 (m) 1425 (m), 1347 (m) (ν_{NO}), 1198 (m), 1140 (s), 1114 (s), 1080 (m), 1042 (m), 808 (m), 625 (m); UV (CH_3CN) λ (nm) (ϵ (M^{-1} cm^{-1})) 650 (680), 583 (820), 554 (870), 375 (9900), 330 (17 500), 273 (14 500). Anal. Calcd for $C_{24}H_{30}O_{12}N_6Cl_2Co{\cdot}CH_3CN{\cdot}H_2O$ (M_r = 724.379 + 41.052 + 18.015): C, 39.86; H, 4.50; N, 12.51. Found: C, 40.83; H, 4.19; N, 12.62.

[Cu(NIT-bpy)·2ClO$_4$] (5). 68%; FAB$^+$ (m-NBA) 630.1 [M − ClO_4 + 2H]$^+$, 612.1 [M − ClO_4 − O], 596.1 [M − ClO_4 − 2O], 529.2 [M − 2ClO_4], 513.2 [M − 2ClO_4 − O], 497.2 [M − 2ClO_4 − 20]; IR (KBr pellet, cm^{-1}) 2978 (m), 1597 (m), 1452 (m), 1425 (m), 1347 (m), 1202 (m), 1140 (s), 1116 (s), 1088 (s), 1049 (s), 807 (m), 625 (m); UV (CH_3CN) λ (nm) (ϵ (M^{-1} cm^{-1})) 702 (540), 590 (1100), 468 (3600), 338 (18 600), 269 (14 100). Anal. Calcd for $C_{24}H_{30}O_{12}N_6Cl_2Cu$ (M_r = 728.992): C, 39.54; H, 4.15; N, 11.53. Found: C, 39.42, H, 4.03, N, 11.42.

[Zn(NIT-bpy)](ClO$_4$)$_2$, CH$_3$CN (6). 95%; FAB$^+$ (*m*-NBA) 651.1/649.1 [M − ClO_4 + 2H]$^+$, 635.1/633.1 [M − ClO_4 + 2H − O], 619.1/

(49) Day, E. P.; Kent, T. A.; Lindahl, P. A.; Münck, E.; Orme-Johnson, W. H.; Roder, H.; Roy, A. *Biophys. J.* **1987**, 52, 837.
(50) Lamchen, M.; Mittag, T. W. *J. Chem. Soc. C* **1966**, 2300.
(51) Parks, J. E.; Wagner, B. E.; Holm, R. H. *J. Organomet. Chem.* **1973**, *56*, 53.

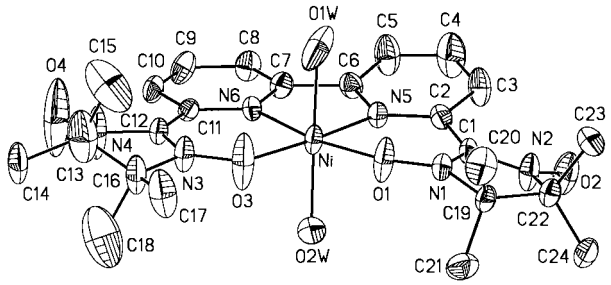

Figure 1. ORTEP view of the $[Ni(NIT\text{-}bpy)\cdot 2H_2O]^{2+}$ cation in complex **1**.

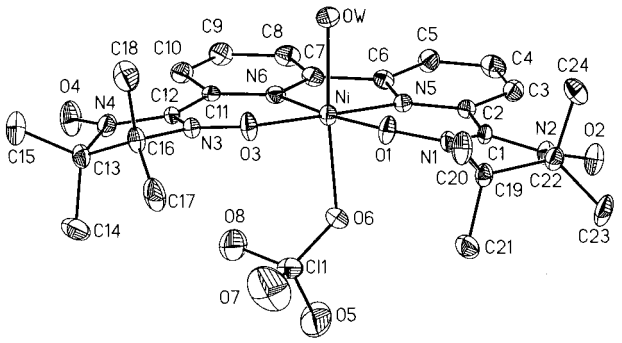

Figure 2. ORTEP view of the $[Ni(NIT\text{-}bpy)\cdot H_2O\cdot ClO_4]^{2+}$ cation in complex **2**

617.1 [M − ClO_4 + 2H − 2O], 551.3/549.3 [M − $2ClO_4$ + H], 535.1/533.1 [M − $2ClO_4$ + H − O], 518.1/516.2 [M − $2ClO_4$ − 2O]; IR (KBr pellet, cm^{-1}) 2986 (m), 1594 (m), 1582 (m), 1455 (m), 1426 (m), 1347 (s), 1268 (m), 1198 (m), 1140 (s), 1116 (s), 1088 (s), 808 (m), 625 (m); UV (CH_3CN) λ (nm) (ϵ (M^{-1} cm^{-1})) 612 (650), 580 (660), 378 (9900), 333 (25 700), 273 (17 600), 234 (31 900), 211 (33 800). Anal. Calcd for $C_{24}H_{30}O_{12}N_6Cl_2Zn\cdot CH_3CN$ (M_r = 730.826 + 41.052): C, 40.46; H, 4.31; N, 12.70. Found: C, 40.35; H, 4.14; N, 12.59.

[Fe(NIT-bpy)]$(ClO_4)_2$, CH_3CN (7). 63%; FAB^+ (*m*-NBA) 641.1 [M − ClO_4 + 2H]$^+$, 625.1 [M − ClO_4 + 2H − O], 609.2 [M − ClO_4 + 2H − 2O], 541.2 [M − $2ClO_4$ + H], 525.0 [M − $2ClO_4$ + H − O], 508.2 [M − $2ClO_4$ − 2O]; IR (KBr pellet, cm^{-1}) 2979 (s), 1560 (m), 1448 (m), 1425 (m), 1384 (s), 1170 (m), 1136 (m), 807 (m), 756 (m); UV (CH_3CN) λ (nm) (ϵ (M^{-1} cm^{-1})) 546 (1200), 350 (6500), 285 (18 700), 217 (44 000). Anal. Calcd for $C_{24}H_{30}O_{12}N_6Cl_2Fe\cdot CH_3CN$ (M_r = 721.292 + 41.052): C, 40.96; H, 4.36; N, 12.86. Found: C, 40.72; H, 4.02; N, 12.55.

Results

Structural Details. The crystal structures of the free NIT-bpy ligand[45] and its complexes **1**−**5** have been determined. In these complexes the NIT-bpy radical behaves as a tetradentate chelate with the two N(bipyridyl) atoms and the O(nitroxyl) atoms making the equatorial plane of a distorted octahedron. Compounds **2**−**4** are isostructural.

[Ni(NIT-bpy)·$2H_2O$]$(ClO_4)_2$ (1). A view of the cation is shown in Figure 1. The nickel(II) cation occupies a distorted octahedral coordination site and is located 0.044 Å above the equatorial plane formed by the N(bipyridyl) atoms and the two O(nitroxyl) atoms of the nitronyl nitroxide radicals. In the equatorial plane, the Ni−N5, Ni−N6, and Ni−O1 bond lengths are similar (average 2.026 ± 0.004 Å) but slightly longer than the Ni−O3 (1.980(9) Å) bond. The N5−Ni−N6 angle shows important deviation from the ideal octahedron (82.3(3)°), presumably due to the geometric constraints of the bipyridyl ring. The axial positions of the octahedron are occupied by two water molecules at 2.08(1) Å.

The relevant geometrical features of the $[Ni(NIT\text{-}bpy)\cdot 2H_2O]^{2+}$ cation which have an impact in the magnetic properties are given hereafter. The Ni−O1−N1 and Ni−O3−N3 angles are 123.5(7) and 126.2(7)°, respectively. The O1−N1−C1−N2−O2 plane containing the unpaired electron has the carbon atom C1 located 0.123 Å from the mean plane and makes an angle of 10.04° with the Ni−O1−N1 plane, 14.54° with the equatorial plane N5−N6−O1−O3, 84.61 and 78.42°, respectively, with the N5−Ow1−O3−Ow2 and N6−Ow1−O1−Ow2 planes, and 22.62° with one bipyridyl ring. On the other hand, the O3−N3−C12−N4−O4 plane is planar and makes angles of 2.04° with the Ni−O3−N3 plane, 1.81° with the equatorial plane N5−N6−O1−O3, 89.63 and 89.68°, respectively, with the N5−Ow1−O3−Ow2 and N6−Ow1−O1−Ow2 planes, and 3.51° with the second bipyridyl ring. The torsion angle between the two pyridine rings is 11.00°. Intermolecular contacts between uncoordinated and neighboring N−O groups are greater than 4 Å (O2- - -O2′, 4.244(8) Å, O4- - -O4′, 4.489(2) Å).

[Ni(NIT-bpy)·H_2O·ClO_4](ClO_4), CH_3CN (2). Figure 2 shows a view of the cation. The coordination sphere around the nickel(II) ion is a distorted octahedron with the nickel(II) ion located 0.013 Å above the equatorial plane formed by the N(bipyridyl) atoms and the O(nitroxyl) atoms. The bond lengths Ni−O1 and Ni−O3 are similar (1.990 Å) but shorter than the Ni−N(bipyridyl) bond lengths (2.016 Å). The N5−Ni−N6 angle shows the greatest deviation from octahedral geometry (82.7°), as observed for **1**. Compound **2** shows a marked difference in apical position compared to compound **1** since one water molecule is axially bound at 2.085 Å while the second axial position is occupied at 2.178 Å by the oxygen atom of a perchlorate anion.

The torsion angle between the two pyridine rings is now only 2.54°. The Ni−O1−N1 and Ni−O3−N3 angles are 122.1(3) and 123.5(3)°, respectively. The O1−N1−C1−N2−O2 system containing the unpaired electron is planar and makes angles of 14.64° with the Ni−O1−N1 plane, 14.20° with the equatorial plane N5−N6−O1−O3, 81.48 and 78.68°, respectively, with the N5−Ow−O3−O6 and the N6−Ow−O1−O6 plane, and 14.29° with one bipyridyl ring. The O3−N3−C12−N4−O4 plane is planar and makes angles of 9.47° with the Ni−O3−N3 plane, 9.43° with the equatorial plane N5−N6−O1−O3, 78.20 and 84.44°, respectively, with the N5−Ow−O3−O6 and the N6−Ow−O1−O6 planes, and 9.56° with the second bipyridyl ring. The shortest intermolecular distances between the uncoordinated N−O groups are greater than 4 Å (O2- - -O2′, 4.354(9) Å).

Finally, the most striking aspect of the packing concerns the short intermolecular distances observed in pairs of centrosymmetrically related $[Ni(NIT\text{-}bpy)\cdot H_2O\cdot ClO_4]^{2+}$ cations. Inside a pair, the two (N5−C2−C3−C4−C5−C6) pyridine rings lie co-parallel with a separation of 3.52 Å. Their C2- - -C5 axis makes an angle of 76.06° with the stacking direction so that the shortest distance observed (C4- - -C2′) is 3.530(9) Å. This arrangement brings the uncordinated N−O group (N2−O2) into close contact with the bipyridyl ring of the centrosymmetrically related cation (O2- -C5′:3.165(8) Å).

[M(NIT-bpy)·H_2O·ClO_4]ClO_4, CH_3CN [M = Mn (3), Co (4)]. The manganese(II) and cobalt(II) compounds (**3**, **4**) are isostructural with **2**. The geometrical features of the cobalt(II) complex remain similar to those of **2**, but this is not so for the manganese(II) compound. Here, the bond lengths of the coordination sphere lie in the expected range for a manganese(II) ion and are significantly longer than those found for the nickel(II) and cobalt(II) complexes; Mn−N(bipyridyl), 2.205 ± 0.004 Å; Mn−Ow, 2.208(6) Å; Mn−O6, 2.249(6) Å; Mn−

Table 2. Selected Data for the Calculated Value Obtained During Parametrization of Magnetic Behavior Obtained for Complexes **1**−**5**

complex	J_{NIT-M} (cm^{-1})		g^a	zJ' (cm^{-1})^b
	J_{12}	J_{23}		
Ni(**1**)	+39.6	−48.7	2.12	−0.3
Ni(**2**)	+27.8	+6.9	2.15	+0.7
Mn(**3**)	−65.3		2.0	+0.2
Co(**4**)	+0.40	−40.3	2.0	+0.2
Cu(**5**)	−166.8		2.02	−1.3

[a] Lande factor. [b] Mean field approximation.

O1, 2.057(4) Å. The Mn−O1−N1 (125.3(3)°) and Mn−O3−N3 (127.4(3)°) angles are also larger. In **3**, the O3−N3−C12−N4−O4 system containing one unpaired electron and the equatorial plane N5−N6−O3−O1 deviate further from coplanarity (17.95°) than in compounds **2** (9.43°) and **4** (9.83°). Also, there is a larger torsion angle (5.17°) between the two rings of the bipyridyl moiety. These subtle differences between the [Mn(NIT-bpy)·H_2O·ClO_4]$^+$cation and **2** or **3** may be ascribed to the larger size of the Mn(II) ion which serves to increase the distance between a pair of [Mn(NIT-bpy)·H_2O·ClO_4]$^+$ cations (3.65 Å) and between the uncoordinated N2−O2 group and the carbon atom of the adjacent bipyridyl ring (O2- -C5′, 3.26 Å).

[Cu(NIT-bpy)·2ClO_4] (5). An ORTEP view is given in Figure S3 (Supporting Information). The copper(II) ion has an elongated octahedral coordination sphere (Jahn−Teller effect) and is located 0.08 Å from the equatorial plane formed by the N(bipyridyl) atoms (Cu−N5: 1.936(7) Å; Cu−N6, 1.955(8) Å) and the two oxygen O(nitroxyl) atoms (Cu−O1, 1.903(7) Å; Cu−O3, 1.913(7) Å). The two perchlorate anions are bonded to the copper(II) ion in axial positions (Cu−O6, 2.517(9) Å; Cu−O10, 2.579(12) Å).

The [Cu(NIT-bpy)]$^{2+}$ cation has a "butterfly" shape and shows greater deviation from planarity than observed for other transition metal ions of this series. The torsion angle between the two pyridine rings is 6.39°. The O1−N1−C1−N2−O2 system containing the unpaired electron is planar and makes angles of 50.85° with the Cu−O1−N1 plane, 31.63° with the equatorial plane N5−N6−O1−O3, and 25.29° with one bipyridyl ring. The O3−N3−C12−N4−O4 plane is planar and makes angles of 27.06° with the Cu−O3−N3 plane, 26.76° with the equatorial plane N5−N6−O1−O3, and 20.43° with the second pyridyl ring. The Cu−O1−N1 and Cu−O3−N3 angles are 117.97(2) and 117.67(3)°, respectively. The shortest intermolecular distance found between the uncoordinated N−O groups is greater than 4 Å (O4- - -O4′, 4.62(2) Å).

Magnetic Properties. The thermal variation of the molar magnetic susceptibility χ has been measured down to 2 K for the NIT-bpy ligand and for complexes **1**−**7**. The results are displayed in the form of χT vs T plots of where T is the absolute temperature. Selected parameters used to fit the magnetic data are gathered in Table 2, and details for the NIT-bpy ligand are given in the Supporting Information.

[Ni(NIT-bpy)·2H_2O](ClO_4)$_2$ (1). The derived value of χT = 1.93 emu K mol^{-1} at room temperature is somewhat smaller than the value (χT = 1.96 emu K mol^{-1}) predicted for uncorrelated spins in the case of a high-spin nickel(II) ($g \approx$ 2.2) and two nitroxide radicals (Figure 3a).

On lowering the temperature, χT decreases slowly, reaching a value of 1.86 emu K mol^{-1} at 220 K. Below this temperature there is a sharp decrease of χT to 1.72 emu K mol^{-1}. It is likely that this sharp breakdown observed around 220 K is due to a phase transition. Then χT decreases regularly but faster than in the high-temperature regime (300−220 K). Between

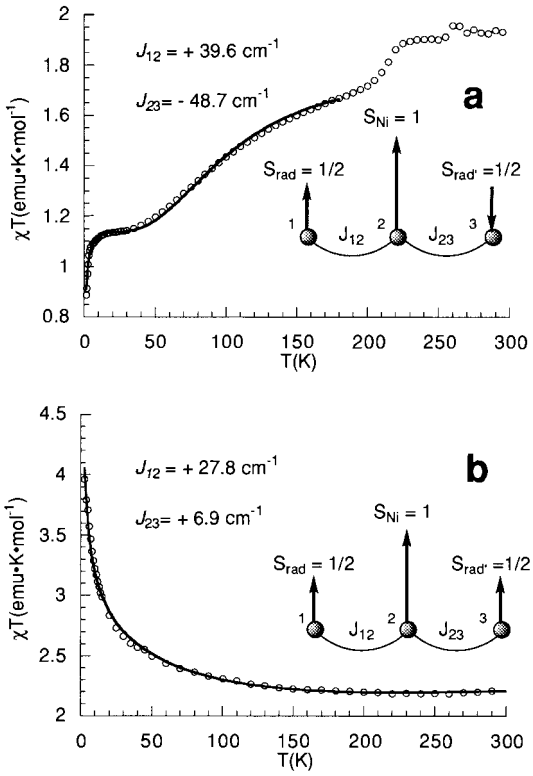

Figure 3. Temperature dependence of the product of the magnetic susceptibility with temperature, χT vs T, for **1** (a) and for **2** (b). The solid line represents the best-fit calculated values. Inset: Magnetic interactions network and values of the coupling constants.

40 and 10 K there is a small plateau at 1.13 emu K mol^{-1}, corresponding to S = 1 (g = 2.2). Finally, at very low temperature the χT product drops dramatically.

The magnetic behavior described here suggests that antiferromagnetic interactions are predominant in compound **1**. At first glance, the value of χT = 1.13 emu K mol^{-1} at low temperature could be explained in either of two ways regarding which exchange coupling pathways are predominant. (i) The main interactions are antiferromagnetic coupling between the nitroxide radicals either through the bipyridyl moiety or through intermolecular interactions, such that at low temperature (40−10 K) we merely observe the paramagnetism of the nickel(II) ion. (ii) The main interactions are those of the central nickel(II) (S = 1) with both nitroxides (S = $^1/_2$) which are indeed different in nature; one radical is ferromagnetically coupled to the nickel(II) ion while the second radical is antiferromagnetically coupled. Indeed, in this case the low-temperature value corresponds to the antiferromagnetic coupling between one spin S = $^3/_2$ and one spin S = $^1/_2$.

Case (i) is easily eliminated since magnetic studies reveals that there was no significative exchange coupling through the bipyridyl moiety[45] and the structure analysis of **1** shows intermolecular contacts which cannot account for the strong antiferromagnetic interactions as would be suggested by the thermal variation of the χT product. Furthermore, the magnetic behavior of **1** is well described in terms of case (ii) with diagonalization of the isotropic Hamiltonian ($H = -2J_{12}S_1S_2 - 2J_{23}S_2S_3$) (see inset to Figure 3a) and with the following values: g = 2.12, J_{12} = +39.6 cm^{-1}, J_{23} = −48.7 cm^{-1}. To take into account the decrease observed below 10 K, we need to introduce into the mathematical model a weak intermolecular

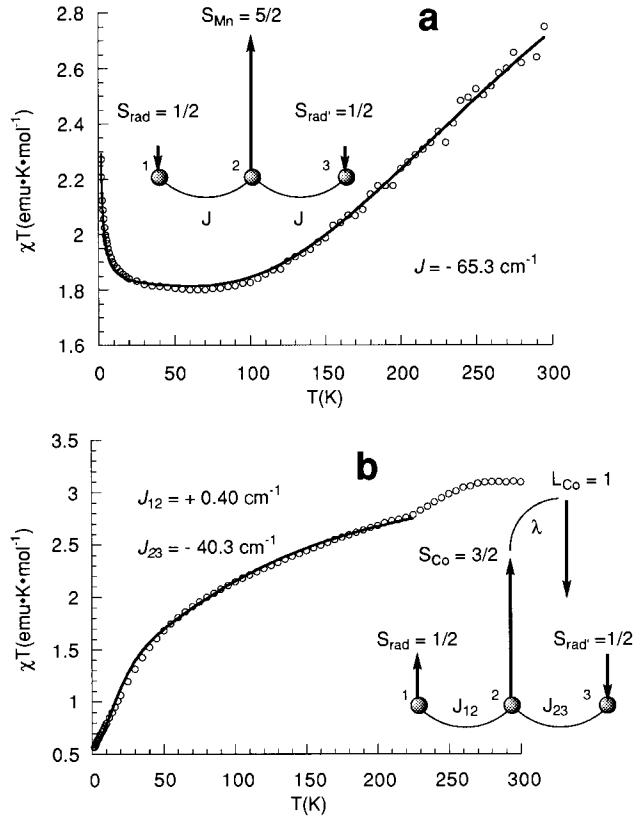

Figure 4. Temperature dependence of the product of the magnetic susceptibility with temperature, χT vs T, for **3** (a) and for **4** (b). The solid line represents the best-fit calculated values. Inset: Magnetic interactions network and values of the coupling constants.

antiferromagnetic interaction based on the mean-field approximation ($zJ' = -0.33$ cm^{-1}).[52]

[Ni(NIT-bpy)·H$_2$O·ClO$_4$]ClO$_4$, CH$_3$CN (2). From a molecular point of view, this nickel(II) compound seems to be similar to **1** but it exhibits quite disparate magnetic properties (Figure 3b). At 300 K the value of $\chi T = 2.22$ emu K mol^{-1} exceeds the value ($\chi T = 1.96$ emu K mol^{-1}) expected for uncorrelated spins arising from octahedral nickel(II) ($g \approx 2.2$) and two nitroxide radicals. Then χT increases continuously with decreasing temperature and reaches a value of 3.96 emu K mol^{-1} at the lowest temperature. This behavior is typical of predominantly ferromagnetic interactions. In addition, the maximum value at low temperature is larger than the theoretical value ($S = 2$, $\chi T = 3.63$ emu K mol^{-1}) expected for two nitroxide radicals ferromagnetically coupled to the nickel(II) atom ($g \approx 2.2$) and suggests that intermolecular ferromagnetic interactions are effective in this compound.

As for **1**, the thermal dependence of the χT product is well described by diagonalization of the isotropic Hamiltonian ($H = -2J_{12}S_1S_2 - 2J_{23}S_2S_3$). The best fit is obtained by taking into account two intramolecular (nickel(II)−nitroxide) ferromagnetic exchange parameters $J_{12} = +27.8$ cm^{-1}, $J_{23} = +6.9$ cm^{-1}, $g = 2.15$ together with a weak ferromagnetic intermolecular interaction related to $zJ' = +0.7$ cm^{-1} (see inset to Figure 3b).

[Mn(NIT-bpy)·H$_2$O·ClO$_4$]ClO$_4$, CH$_3$CN (3). The value of $\chi T = 2.75$ emu K mol^{-1} at room temperature is much lower than the value ($\chi T = 5.13$ emu K mol^{-1}) expected for uncorrelated spins in the case of a high-spin manganese(II) ($g \approx 2.0$) and two nitroxide radicals (Figure 4a). On lowering the temperature, χT falls rapidly to a constant value of 1.80 emu K mol^{-1}, corresponding exactly to a spin $S = {}^3/_2$. Below 40 K, it increases continuously and reaches a value of 2.27 emu K mol^{-1} at the lowest temperature (1.8 K).

Above 50 K, the magnetic behavior indicates that very strong antiferromagnetic interactions are effective between the two radicals and the manganese(II) ion ($S = {}^3/_2$, $\chi T = 1.80$ emu K mol^{-1}). The increase of χT at low temperature is attributed to the intermolecular ferromagnetic interactions, as observed for the isostructural nickel(II) compound **2**. In this case, the thermal variation of the χT product is best fitted by using an "effective" exchange coupling parameter, J, in the isotropic Hamiltonian ($H = -2J(S_1S_2 + S_2S_3)$) and considering an intermolecular interaction, zJ', based on the mean-field approximation. The best fit was obtained using the following parameters: $J = -65.3$ cm^{-1}, $g = 2.0$, $zJ' = +0.22$ cm^{-1} (see inset to Figure 4a).

[Co(NIT-bpy)·H$_2$O·ClO$_4$]ClO$_4$, CH$_3$CN (4). At room temperature the χT product is equal to 3.10 emu K mol^{-1}, leading to a contribution of 2.35 emu K mol^{-1} for the isolated cobalt(II) cation. This value is much higher than that calculated from the "spin-only" equation ($\chi T = 1.875$ emu K mol^{-1}). Lowering the temperature causes a sharp decrease of the χT product around 250 K (Figure 4b). Then, χT decreases continuously with decreasing temperature from 225 K ($\chi T = 2.79$ emu K mol^{-1}) to 2 K ($\chi T = 0.57$ emu K mol^{-1}).

Two important findings emerge from these results. First, the orbital degeneracy of Co(II) has to be included in the model for a correct interpretation of the data. Second, antiferromagnetic interactions are dominant for this compound. However, the value of χT at 2 K is somewhat higher than that expected for a $S = {}^1/_2$ ground-state arising from antiferromagnetic coupling between the Co(II) Kramers doublet and the two radicals. Clearly, an intermolecular ferromagnetic interaction should be taken into account here as was the case for the isostructural nickel(II) and manganese(II) compounds **2**−**3**. With this in mind, the Hamiltonian ($H = -2J_{12}S_1S_2 - 2J_{23}S_2S_3 - ({}^3/_2)k\lambda L_{Co}S_{Co} + DL^2_{z(Co)}$) was used in the calculation of the matrix elements from the 48 $|M_{L_1}, M_{S_1}, M_{S_2}, M_{S_3}\rangle$ functions. After diagonalization of the matrix, the thermal variation of the χT product over the temperature range 2−225 K was fitted by using the MINUIT subroutine. Only J_{12}, J_{23}, and zJ' (intermolecular interaction) were considered. The parameters k, λ, and D were allowed to vary over a small range around the free-ion ($k = 1$, $\lambda = -245$ K) values, and D was taken as reported previously.[53] The best fit was obtained after considering two different exchange interaction parameters: a negative one ($J_{23} = -40.3$ cm^{-1}) and one close to zero ($J_{12} = +0.40$ cm^{-1}). Slight variations in the value of this latter parameter led to a significant departure from the experimental data. The remaining parameters were found to be $zJ' = +0.24$ cm^{-1}, $g = 2.0$, $k = 0.95$, $\lambda = -163.3$ cm^{-1}, and $D = 1320.5$ cm^{-1}.

[Cu(NIT-bpy)·2ClO$_4$] (5). The χT product at room temperature (0.60 emu K mol^{-1}) is well below the value expected for three uncorrelated spins $S = {}^1/_2$ (Figure 5a) and decreases rapidly as the sample is cooled, reaching a plateau around 100 K ($\chi T = 0.38$ emu K mol^{-1}) that corresponds to $S = {}^1/_2$. At temperatures below 20 K, a sharp and irreversible decrease of χT is observed.

As for **1**, intramolecular spin pairing of the radicals is not expected to play a role here and the constant value observed below 100 K arises from strong antiferromagnetic coupling between the radicals and the copper(II) ion, resulting in a ground

(52) O'Connor, C. J. *Prog. Inorg. Chem.* **1982**, *29*, 203.

(53) Kahn, O.; Tola, P.; Coudanne, H. *Chem. Phys.* **1979**, *42*, 355.

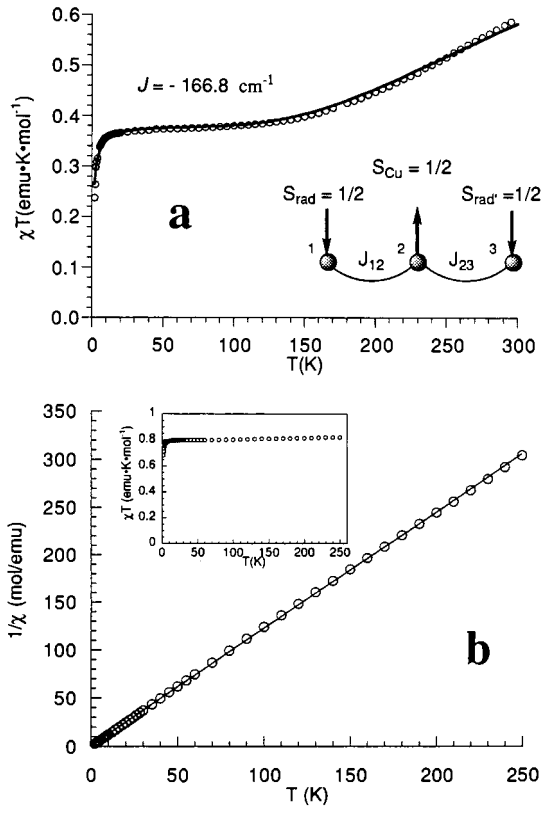

Figure 5. (a) Temperature dependence of the product of the magnetic susceptibility with temperature, χT vs T, for **5**. The solid line represents the best-fit calculated values. Inset: Magnetic interactions network and values of the coupling constants. (b) Temperature dependence of the reciprocal susceptibility, $1/\chi$ vs T, for compounds **7**. The solid line represents the best-fit calculated values. Inset: χT vs T curves.

term with effective spin $S = {}^1/_2$. A good fit was obtained using $J = -166.8$ cm^{-1}, $g = 2.016$, and an antiferromagnetic intermolecular interaction $zJ' = -1.3$ cm^{-1}.

[M(NIT-bpy)·H$_2$O·ClO$_4$]ClO$_4$, CH$_3$CN [M = Zn (6), Fe (7)]. The zinc(II) and iron(II) complexes exhibit similar thermal variation of the χT product, corresponding to two quasi-isolated $S = {}^1/_2$ spins. This behavior is expected for a diamagnetic metal ion. In the case of the ferrous complex, this means that the iron(II) cation is in the diamagnetic low-spin state. In both cases, the decrease of χT observed at temperatures below 20 K can be attributed to weak intermolecular interactions. Thus, the reciprocal susceptibility of both compounds (Figure 5b) follows a Curie−Weiss law with $\theta = -2.43$ and -0.51 cm^{-1} for **6** and **7**, respectively.

Discussion

Theoretical calculations and polarized neutron diffraction studies of nitronyl nitroxide radicals[54] and their complexes[55] provide a good indication of the expected spin-density distribution of the NIT-bpy biradical in the present compounds. Thus, we do not expect the bipyridine unit bridging the two radicals to mediate any sizable magnetic interaction in the free NIT-bpy biradical or in complexes **1**−**7**. This is ascertained by the magnetic susceptibility measurement of the biradical in frozen and dilute solution. Furthermore, the magnetic behavior of the diamagnetic zinc(II) and iron(II) complexes indicates little or no intramolecular magnetic coupling between the two radicals. Consequently, the antiferromagnetic behavior noted for the crystalline ligand is due to spin pairing between the nitronyl nitroxide radicals of neighboring molecules. Indeed, packing of the free ligand shows the N−O groups to be at short distances and oriented in a head-to-tail fashion. This arrangement favors antiferromagnetic interactions.[21] Moreover, intermolecular interaction in these centrosymmetric systems is at a maximum when the two NO groups are arranged such a way that the O−N−O′ angle (α) is equal to 90° and the angle (β) between the π^* orbitals of the nitronyl nitroxide radicals with a vector normal to the N_2O_2 plane is also 90°. This situation corresponds to maximum σ overlap between the π^* orbitals. For the NIT-bpy biradical we found $\alpha = 83.7°$ and $\beta = 89.3°$. This situation should promote strong interactions as indeed observed ($J = -16.7$ cm^{-1}) despite the fact that the NO subunits are separated at 3.697 Å.

The magnetic properties of copper(II)−nitroxide complexes have been reviewed.[20,21] The copper(II)−nitroxide magnetic interaction is markedly dependent on the copper(II) coordination geometry and may be either ferro- or antiferromagnetic. All manganese(II) complexes reported to date exhibit antiferromagnetic metal−nitroxide[33,56,57] interactions, as observed here for compound **3**. In the case of nickel(II), compounds **1** and **2** provide the first known examples having large ferromagnetic exchange interactions between a nitronyl nitroxide and a nickel(II) ion.[58,59] Such behavior was previously observed only in nickel(II)−imino nitroxide complexes.[60] The cobalt(II) compound **4**, one of the few examples of cobalt(II)−nitroxide complexes,[59] is isostructural with the nickel(II) and manganese(II) compounds **2** and **3** and exhibits a thermal variation of the magnetic susceptibility which can be fit on the basis that one of the cobalt(II)−nitroxide magnetic interactions is weakly ferromagnetic. For compounds **2**−**4**, the magnetic behavior is explanable only after taking into account an additive intermolecular ferromagnetic interaction. We present now a unified picture of the magnetic properties of these various metal complexes. For clarity we will discuss separately the intra- and intermolecular aspects of the magnetic behavior.

Intramolecular Interactions. Our understanding of the metal−nitroxide interactions In compounds **1**−**5** relies on simple molecular-orbital considerations. In this frame the observed coupling constant J is considered as the sum of individual contributions J_{ir} involving each pair of magnetic orbitals implicated in the exchange phenomena[61]

$$J = (1/N_m)\sum_{i=1}^{N_m} J_{ir}$$

where N_m is the number of unpaired electrons associated with the metal ion, i and r being the metal (d) and radical (π^*) magnetic orbitals. Each individual J_{ir} contribution has a ferro

(54) Zheludev, A.; Barone, V.; Bonnet, M.; Delley, B.; Grand, A.; Ressouche, E.; Rey, P.; Subra, R.; Schweizer, J. *J. Am. Chem. Soc.* **1994**, *116*, 2019.
(55) Ressouche, E.; Boucherle, J. X.; Gillon, B.; Rey, P.; Schweizer, J. *J. Am. Chem. Soc.* **1993**, *115*, 3610.
(56) Caneschi, A.; Gatteschi, D.; Rey, P.; Sessoli, R. *Inorg. Chem.* **1991**, *30*, 3936.
(57) Caneschi, A.; Gatteschi, D.; Laugier, J.; Pardi, L.; Rey, P.; Zanchini, C. *Inorg. Chem.* **1988**, *27*, 2027.
(58) Caneschi, A.; Gatteschi, D.; Renard, J. P.; Rey, P.; Sessoli, R. *Inorg. Chem.* **1989**, *28*, 2940.
(59) Caneschi, A.; Gatteschi, D.; Laugier, J.; Rey, P.; Sessoli, R. *Inorg. Chem.* **1988**, *27*, 1553.
(60) Luneau, D.; Rey, P.; Laugier, J.; Belorizky, E.; Cogne, A. *Inorg. Chem.* **1992**, *31*, 3578.
(61) (a) Hay, P. J.; Thibeault, J. C.; Hoffmann, R. *J. Am. Chem. Soc.* **1975**, *97*, 4884. (b) Kahn, O. *Struct. Bond. (Berlin)* **1987**, *68*, 89.

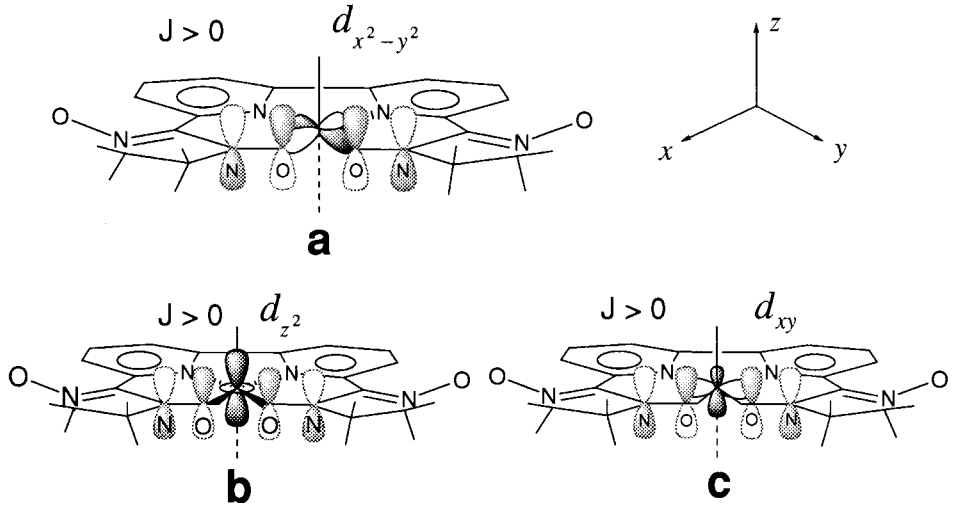

Figure 6. Representation of the magnetic orbitals for each center for a planar conformation of the ligand.

J_{ir}^{F} and an antiferromagnetic J_{ir}^{AF} component[62]

$$J_{ir} = J_{ir}^{AF} + J_{ir}^{F} \quad \text{or} \quad J_{ir} = 2\beta S_{ir} + K_{ir}$$

where βS is the product (J_{ir}^{AF}) of a resonance integral with an overlap integral S, and K is the bielectronic exchange integral (J_{ir}^{F}). Keeping this in mind, we assume that the extent of overlap between metal and radical magnetic orbitals reflects the magnitude of the antiferromagnetic component, whereas orthogonality (or symmetry-forbidden) overlap of the same orbitals will induce a ferromagnetic contribution.

A representation of the overlap between the magnetic orbitals associated, respectively, with the radical (π^*) and metal centers is given in Figure 6. This refers to the [ideal] case where the N_2O_2 ligand adopts a planar conformation similar to that found in Schiff-base complexes of C_{2v} symmetry.[63] This particular arrangement causes the metal $d_{x^2-y^2}$ orbital to become orthogonal to the radical orbitals (Figure 6a). Moreover, overlap between the radical (π^*) orbitals and the metal d_{z^2} and d_{xy} orbitals is symmetry forbidden (Figure 6b,c). This provides the basis for ferromagnetic interactions in these complexes. However, slight deviations from this ideal case and/or contributions from the d_{xz} and d_{yz} metal orbitals could result in antiferromagnetic behavior.

In the copper(II) complex **5** the O−N−C−N−O mean planes of the two radicals make angles of 31.6 and 26.8° with the equatorial plane of the octahedral copper ion. This geometry favors overlap of the half-filled π^* orbital of the nitroxide radical with the $d_{x^2-y^2}$ magnetic orbital of copper(II) and is responsible for the strong antiferromagnetic copper(II)−nitroxide interaction ($J = -166.8$ cm^{-1}). The manganese(II)−nitroxide complexes, owing to the symmetry of the five d orbitals, always involve a sizable overlap between magnetic orbitals. Therefore, the manganese(II)−nitroxide interaction is antiferromagnetic regardless of geometry and the correlation between structure and metal−nitroxide exchange coupling can be rationalized in terms of extended Hückel calculations.[57] The short Mn−O(nitroxide) bond lengths and the value of the Mn−O1−N1 and Mn−O2−N2 angles contribute to the strong antiferromagnetic exchange coupling found for **3**.

Although ferromagnetic interactions have not before been observed for nickel(II) nitronyl nitroxide complexes, they are not unexpected. Indeed, this must happen whenever the plane containing the conjugate group ONCNO is coplanar with the equatorial plane of an octahedral nickel(II) ion because, in this geometry, the π^* radical orbital is strictly orthogonal with the $d_{x^2-y^2}$ while its overlap with the d_{z^2} orbital is symmetry-forbidden (Figure 6a and b, respectively). The result is that the two components of the magnetic coupling corresponding to both $\pi^*-d_{x^2-y^2}$ and $\pi^*-d_{z^2}$ interactions become ferromagnetic. Let us now consider the case where the planes are not coplanar, as is the situation found here for the nickel(II) complexes **1** and **2**. Two relevant geometrical parameters have to be considered; namely, (i) the two dihedral angles that the radical plane ONCNO makes with the equatorial plane (*xy*) on one side and (ii) the two planes (*xz*, *yz*) which lie perpendicular to the equatorial plane on the other side. The deviation of these angles from 0 or 90° controls the extent to which the radical π^* orbital will overlap with $d_{x^2-y^2}$ or d_{z^2} nickel(II) magnetic orbitals.

To further test this assumption we have made a critical comparison of the two nickel(II) compounds. Despite different packings, the two cations $[Ni(NIT\text{-}bpy)\cdot 2H_2O]^{2+}$ (**1**) and $[Ni(NIT\text{-}bpy)\cdot H_2O\cdot ClO_4]^{+}$ (**2**) are structurally similar but magnetically distinct. Whereas in **1**, both ferro- and antiferromagnetic exchange couplings are effective we only observe ferromagnetic interactions in **2**. Therefore, it is likely that subtle modifications around the nickel core, as induced by different ancilliary ligands, are responsible for these magnetic divergences.

In **1**, the radical plane O3−N3−C12−N4−O4 is coplanar with the equatorial plane N6−N5−O1−O3, this geometry leading to zero overlap between the magnetic orbitals. Consequently, we attribute the strong ferromagnetic coupling constant ($J_{12} = +39.6$ cm^{-1}) to the magnetic interaction between the nickel(II) and the radical corresponding to the O3−N3−C12−N4−O4 plane. Concerning the second radical, the O1−N1−C1−N2−O2 plane is not coplanar with the equatorial plane but remains perpendicular to the N5−Ow1−O3−Ow2 and N6−Ow1−O1−Ow2 planes (*xz*, *yz*). In this geometry, the π^* radical orbital overlaps only with the $d_{x^2-y^2}$ nickel(II) orbital and not with the d_{z^2} orbital. This induces anti- and ferromagnetic components which combine to give the observed magnetic interaction. In **1**, the nickel(II)−nitroxide coupling constant is of antiferromagnetic character ($J_{23} = -48.7$ cm^{-1}), indicating that the component due to the $\pi^*-d_{x^2-y^2}$ orbital interaction dominates.

In **2**, both radical planes lie outside the equatorial plane containing the bipyridine but remain perpendicular to the N5−

(62) Kahn, O.; Briat, B. *Faraday Trans.* **1976**, *72*, 268.
(63) Daul, C.; Schläpfer, C. W.; von Zelewsky, A. *Struct. Bond. (Berlin)* **1979**, *36*, 129.

Ow−O3−O6 and N6−Ow−O1−O6 planes (*xz*, *yz*). In this complex the ferromagnetic component due to the $\pi^*-d_{z^2}$ interaction prevails over the $\pi^*-d_{x^2-y^2}$ components. The larger calculated value $J_{12} = +27.8$ cm^{-1} may be reasonably ascribed to the interaction of the nickel(II) ion with the radical plane O3−N3−C12−N4−O4, that shows the least deviation from the equatorial plane. This is in agreement with the highest value $J_{12} = +39.6$ cm^{-1} found for **1** which corresponds to the ideal coplanar case. The larger deviation of the O1−N1−C1−N2−O2 plane from coplanarity with the equatorial plane is also in agreement with the smaller ferromagnetic interaction ($J_{23} = +6.9$ cm^{-1}) in **2**. This value seems to be in disagreement with the strong antiferromagnetic value ($J_{23} = -48.7$ cm^{-1}) found in complex **1**. The exact reasons for this difference remain obscure. It should be recalled, however, that the antiferromagnetic coupling value ($J_{23} = -48.7$ cm^{-1}) for **1** has been obtained after simulation of the magnetic susceptibility below the small break (200 K) observed on the experimental curve (Figure 3a). At high temperature the χT product decreases more slowly with decreasing temperature, indicating that the antiferromagnetic interaction corresponding to the room-temperature structure is smaller than that obtained below 200 K. Furthermore, the small ferromagnetic interaction found ($J_{23} = +6.9$ cm^{-1}) for **2** indicates that we are in a critical domain where minor variations of the geometrical parameters may increase significantly the overlap of the magnetic orbitals, overcoming the ferromagnetic contribution.

In the case of the cobalt(II) complex **4**, a good agreement between theory and experiment was obtained by considering the orbital degeneracy of the Co^{2+} cation. One of the cobalt(II)-nitroxide interactions was found to be weakly ferromagnetic ($J_{12} = +0.40$ cm^{-1}). The strong antiferromagnetic interactions expected between the $d_{yz}-\pi^*$ and $d_{xz}-\pi^*$ orbital overlap are attenuated in the Co complex since, in a elongated octahedral environment, these orbitals are slightly stabilized with respect to the d_{xy} orbital. Consequently, the appropriate cobalt(II) magnetic orbitals are $d_{x^2-y^2}$, d_{z^2}, and d_{xy}, and the explanation we gave for the isostructural [and geometrically identical] compound **2** is also valid in this case, but we have now to consider additional weak ferro and antiferromagnetic components due to the π^*-d_{xy} interaction.

Intermolecular Interaction. In the manganese(II) complex **3** the high-temperature antiferromagnetic behavior is ascribed to manganese(II)−nitroxide exchange interaction, suggesting that the ferromagnetic-like behavior observed at low temperature should be correlated to the crystal packing. This assumption is corroborated by the magnetic behavior of the isostructural nickel(II) and cobalt(II) compounds **2** and **4** which are correctly interpreted only if we take into account an intermolecular ferromagnetic interaction. On the other hand, comparison of the crystal packing of the nickel(II) compounds **1** and **2** illustrates the features responsible for the disparity in intermolecular magnetic interactions. Indeed, in **1** and **2**, the shortest intermolecular distances between the uncoordinated N−O groups remain similar and are not expected to have a strong impact on the magnetic behavior. It is likely, therefore, that the intermolecular ferromagnetic interaction involves the so-called McConnell's spin polarization mechanism I,[64,65] due to the peculiar cation pairing found in the isostructural compounds **2**−**4**.

On the basis of theoretical calculations and polarized neutron diffraction studies made for related nitronyl nitroxides and their

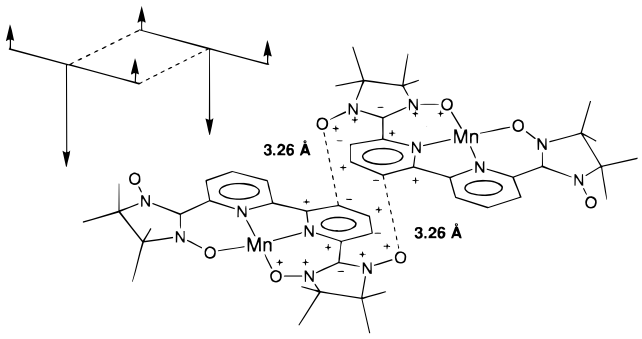

Figure 7. View showing the arrangement of two centrosymmetrically related $[Mn(NIT\text{-}bpy)\cdot H_2O\cdot ClO_4]^{2+}$ cation in complex **3.** The + and − represent positive and negative spin densities, respectively.

complexes, we suppose that the spin-density distribution is mainly localized over the two NO groups in our compounds. In addition, a large negative contribution appears on the sp^2 central carbon atom and there is weak alternative delocalization over the bipyridyl rings (Figure 7). Therefore, the close proximity (3.16−3.26 Å) between the bipyridyl rings (N5−C2−C3−C4−C5−C6) of the paired $[M(NIT\text{-}bpy)\cdot H_2O\cdot ClO_4]^+$ (M = Ni(II), Mn(II), Co(II)) cations in compounds **2**−**4** offers potential pathways for intermolecular magnetic interactions involving the spin polarization effect, via McConnell's mechanism. First, considering only the superimposition of carbon atoms C2 and C4i ($i = -x, -y, -z$) which carry small and equivalent positive spin densities (Figure 7), we would expect weak antiferromagnetic exchange interactions. This is certainly not the major pathway for intermolecular ferromagnetic interaction. On the other hand, pairing of the cations $[M(NIT\text{-}bpy)\cdot H_2O\cdot ClO_4]^+$ (M = Ni(II), Mn(II), Co(II)) brings an uncoordinated N−O group carrying a large positive spin density in close proximity to the carbon atom (C5i) that carries a small negative spin density (O2- - -C5i = 3.165(8) Å (**2**) and 3.255(8) Å (**3**), $i = -x, -y, -z$). Owing to the spin polarization effect, we would expect to observe ferromagnetic coupling. Such intermolecular interactions have been invoked to justify ferromagnetic coupling in some nitroxide radicals and their complexes.[37,66]

Due to the small fraction of negative spin density expected on C5, the magnitude of intermolecular ferromagnetic interaction should be weak. This situation is apparent from the experimental determination of the intermolecular exchange coupling parameters. However, because it also involves high spin density on the N−O units it should be sufficient to overcome all other possible intermolecular antiferromagnetic interactions, such as might arise from stacking of the bipyridyl rings. It is also worthy to note that, at least for the Mn(II) complex an antiferromagnetic interaction between the metal center and one radical belonging to the adjacent "paired" molecule leads also to a net increase of χT product at low temperature. Thus, for **3** the behavior is best described as ferrimagnetic (see inset Figure 7).

Conclusion

Structural and magnetic properties have been described for a series of complexes comprising the NIT-bpy ligand and a first-row transition metal with electronic configuration ranging from d^5 to d^{10}. The structural studies show that, from the coordination point of view, the 2,2′-bipyridyl-*N*-oxide-*N*-oxyl biradical is a

(64) McConnell, H., M. *J. Chem. Phys.* **1963**, *39*, 1910.
(65) Kollmar, C.; Kahn, O. *Acc. Chem. Res.* **1993**, *26*, 259.
(66) Izuoka, A.; Fukada, M.; Kumai, R.; Itakura, M.; Hikami, S.; Sugawara, T. *J. Am. Chem. Soc.* **1994**, *116*, 2609.

versatile tetradendate chelating ligand that readily coordinates each transition metal ion. The manganese(II) complex **3** exhibits the expected Mn(II)−nitroxide antiferromagnetic interactions, but an intermolecular ferromagnetic coupling is also apparent at low temperature. This interaction (which pertains to the isostructural compounds **2** and **4**) is assigned to spin-polarization effects arising because of close contact between uncoordinated N−O groups and carbon atoms of the bipyridyl rings carrying opposite spin density. For the first time, large Ni(II)−nitroxide ferromagnetic interactions are observed. They are the consequence of the conformation of the biradical which, when coordinated to the metal ion the magnetic orbitals appear to move away from being co-extensive within a planar environment. We have shown that the magnitude of the interaction in compounds **1** and **2** is strongly correlated with structural features. Complex **4** is a rare example of a cobalt−nitroxide system for which a complete treatment of the magnetic susceptibility has been performed, and it is important to realize that spin−orbit coupling terms cannot be neglected.

These complexes document the intimate relationship between magnetic properties and structural features, thereby enabling some concluding remarks to be made. We see that crystal packing may be an effective way to mediate ferromagnetic interaction but the importance of this effect is difficult to predict. On the other hand, the most significant result to emerge from this work is certainly the evidence that, by proper design of the radical ligand, it is possible to obtain ferromagnetic nickel(II)−nitroxide compounds. This was hitherto the sole province of copper(II)−nitroxide complexes.[67]

Acknowledgment. The authors are grateful to Dr. Gilles Ulrich for the preparation of a NIT-bpy sample and are pleased to acknowledge continued technical assistance from Richard Poinsot and Prof. Antoine Herr and helpful discussions with Prof. Anthony Harriman, Dr. Marc Drillon, Dr. Paul Rey, and Dr. Pierre Rabu. This work was partially supported by the CNRS, the Engineer School of Chemistry (ECPM), and by the Human Capital and Mobility Program of the EU (Network: "Magnetic Molecular Materials", ERBCHRXCT 920080).

Supporting Information Available: Synthetic details with preparation Schemes 1 and 2, structural details and magnetic properties of NIT-bpy ligand (Figures S1 and S2), structural details of complex **5** (Figure S3), magnetic properties of complex **6** (Figure S4), details of data collection and structure refinement (Tables S1−S6), positional parameters (Table S7−S12), calculated positions of hydrogen atoms (Tables S13−S18), complete listing of bond lengths (Tables S19−S24), bond angles (Tables S25−S30), anisotropic thermal parameters (Tables S31−S36), and summary of the crystal structural data collection and refinement and angles between selected planes in complexes **1**−**5** are available (54 pages). Ordering information is given on any current masthead page.

IC9803412

(67) Gatteschi, D.; Laugier, J.; Rey, P.; Zanchini, C. *Inorg. Chem.* **1987**, *26*, 938.